The anomalous structure factor of dense star polymer solutions

M Watzlawek†, H Löwen†‡ and C N Likos‡

† Institut für Theoretische Physik II, Heinrich-Heine-Universität Düsseldorf, Universitätsstraße 1, D-40225 Düsseldorf, Germany
‡ Institut für Festkörperforschung, Forschungszentrum Jülich GmbH, D-52425 Jülich, Germany

Abstract. The core–core structure factor of dense star polymer solutions in a good solvent is shown theoretically to exhibit an unusual behaviour above the overlap concentration. Unlike usual liquids, these solutions display a structure factor whose first peak decreases with increasing density while the second peak grows. The scenario repeats itself with the subsequent peaks as the density is further enhanced. For low enough arm numbers f ($f \leqslant 32$), various different considerations lead to the conclusion that the system remains fluid at all concentrations.

1. Introduction

Star polymers are macromolecular entities consisting of f polymeric arms chemically attached to a common centre. At the limit where the number of monomers per arm (degree of polymerization) N is large, the size of the central core of the star is negligible compared with the overall radius of the macromolecular aggregate and can be ignored at a first approximation. Scaling theory has provided insight into the structure and conformation of a *single* star and the way that these properties are influenced by the arm number (functionality) f, N and solvent quality [1, 2]. From both theoretical and experimental points of view, it is even more interesting to describe the properties of *dense* star polymer solutions by means of an effective pair potential acting between star centres. Experimentally, this is important as interstar correlations are ubiquitous in attempts to understand neutron scattering spectra of dense star polymer solutions. Moreover, such a description of stars establishes a bridge between polymer and colloidal science: indeed, due to their peculiar construction, star polymers can be viewed as hybrids between polymers and colloidal particles. Once such a description has been established, it is then possible to look at a star polymer solution as an effective one-component system of point particles (the star centres) and employ the known machinery from liquid-state theory and/or computer simulations to study its properties.

   By way of direct comparison with experimental data, it was found recently that star polymers in a good solvent can be described by an effective pair potential which is logarithmic for short distances and crosses over to a Yukawa form for larger interstar separations [3]. This is a new type of interaction in the sense that (i) it has an ultra-soft logarithmic core whose hardness depends in fact on the functionality f in a way which will be explained shortly and (ii) it features a crossover from one functional form to another at some length scale σ which is of the order of the corona diameter of the star. Systems which are described by simple, spherically symmetric interactions have been

studied extensively in the last thirty years, since the development of powerful computers made integral equation theories and simulations computationally tractable [4–6]. For most of the commonly considered interactions (power laws, Yukawa, square-well or square-shoulder potentials etc) the liquid structure factor $S(k)$ features a single characteristic length which is basically set by the density. Moreover, the correlations in structure grow with increasing density ρ until, at some temperature-dependent value, the system crystallizes. We call the liquids for which such a scenario materializes *usual* or *normal*. The purpose of this paper is to show that star polymer solutions are unusual, in the sense that $S(k)$ or its real-space counterpart, the radial distribution function $g(r)$, have quite unexpected behaviour above the overlap concentration of the solution. The latter is defined as the polymer concentration at which the stars start overlapping within their corona. There exist two competing length scales which manifest themselves in the form of a structure factor whose peaks do not grow simultaneously in height as ρ increases, but rather lower-order peaks grow higher until they completely dominate and the original main peak disappears. These two lengths are the average interparticle distance $a \propto \rho^{-1/3}$ and the corona diameter σ of the stars. Moreover, for low enough functionality, freezing does not take place, i.e., the system remains fluid at all densities.

The rest of the paper is organized as follows. In section 2 we present the model pair potential and briefly discuss its properties. In section 3 we present results from computer simulations and integral equation theories regarding the structure of the system for a very wide range of densities demonstrating the unusual features and we discuss their origin. In section 4 we present a simple 'hard-sphere mapping' argument to establish the limit of f beyond which the system does not crystallize. In section 5 we discuss the connection with experiments. Finally, in section 6 we summarize and conclude.

2. The pair potential acting between star polymers

Our starting point is the pair potential acting between two star polymers in a good solvent separated by a centre-to-centre distance r, which reads

$$\frac{V(r)}{k_B T} = \begin{cases} (5/18)\, f^{3/2}\left[-\ln(r/\sigma) + (1 + \sqrt{f}/2)^{-1}\right] & (r \leqslant \sigma) \\ (5/18)\, f^{3/2}(1 + \sqrt{f}/2)^{-1}(\sigma/r) \exp[-\sqrt{f}(r - \sigma)/2\sigma] & (r > \sigma) \end{cases} \tag{1}$$

where k_B is Boltzmann's constant and T is the absolute temperature. This is an entropic interaction stemming from excluded-volume effects between monomers belonging to two different stars in a good solvent. It was shown recently [3] that the length scale σ has to be chosen as twice the distance between the centre of the star and the centre of the largest (outermost) blob [7]. The logarithmic form of the interaction for interparticle distances $r < \sigma$ results from the arguments of Witten and Pincus [8]. For $r > \sigma$ we take an exponential form for the interaction with a decay length equal to the largest blob diameter. For details on the determination of the overall numerical prefactor of the logarithmic term, we refer the reader to reference [3]. The amplitude of the Yukawa tail is finally determined by the requirement of smoothness of the interaction at $r = \sigma$. In what follows we use σ as the unit of length and introduce a dimensionless 'packing fraction' η defined as

$$\eta \equiv \frac{\pi}{6}\rho\sigma^3. \tag{2}$$

It has been shown in reference [3] that this choice of a pair potential [9] brings about good agreement between theory and experiment as regards small-angle neutron scattering (SANS) data for a wide range of densities (or polymer volume fraction). Moreover, a
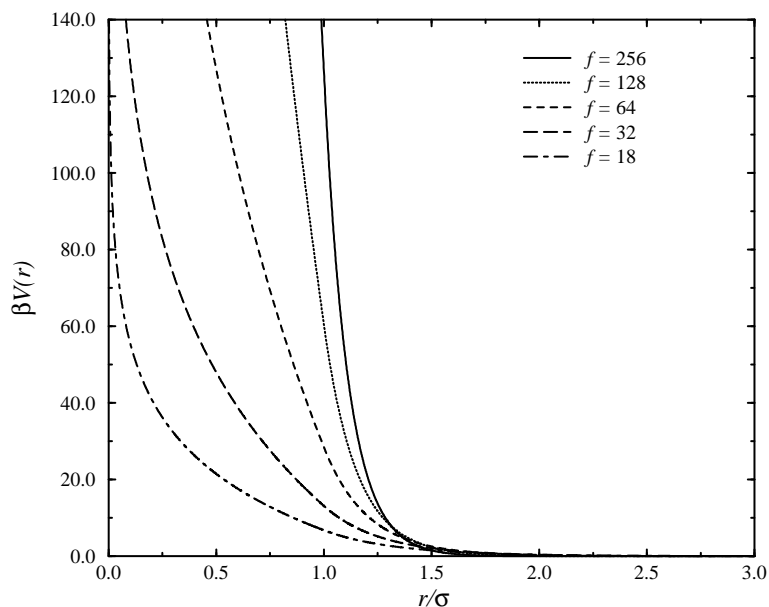
Figure 1. The pair potential given by equation (1) for $f = 18, 32, 64, 128$ and 256 as a function of the centre-to-centre separation r.

similar exponential 'cut-off' of the logarithmic part of the interaction has also been employed recently in a study of the elastic moduli of block copolymer micelles [10]. The entropic nature of the interaction renders the temperature T irrelevant, as the Boltzmann factor $e^{-\beta V(r)}$ is temperature independent. Instead, the arm number f plays now the role of an effective inverse temperature. Indeed, in the limit $f \to 0$ the interaction vanishes, whereas at the 'colloidal limit' $f \to \infty$ we recover the well-known hard-sphere (HS) interaction. In figure 1 we show the pair potential for different values of f. Whereas for large $f = 128$ and 256 there is a spectacular change in its behaviour as r crosses σ, for low f-values, the potential is ultra-soft and its range becomes longer.

As will be shown in section 4, the ultra-soft character of the interaction at hand has the consequence that, for low enough values of the functionality f, the system never crystallizes, no matter how large the density or external pressure are. Thus, this system offers us a unique possibility to examine the behaviour of the structural functions of the liquid (the radial distribution function and/or the structure factor) over a practically unlimited range of densities. This is the subject of the following section.

3. The anomalous structure factor

First, we summarize some basic notions from the theory of classical liquids and refer the reader to reference [4] for details. A quantity of central interest for a classical fluid in equilibrium is the so-called radial distribution function $g(r)$ and the closely associated pair correlation function $h(r) \equiv g(r) - 1$. If we call ρ the number density of the liquid, then the quantity $\rho g(r)$ is nothing else but the density profile that develops if we keep a particle fixed at the origin. In other words, the quantity $g(r)$ expresses the ordering of the rest of the system around a given particle of the liquid. Equivalently, one can look at the
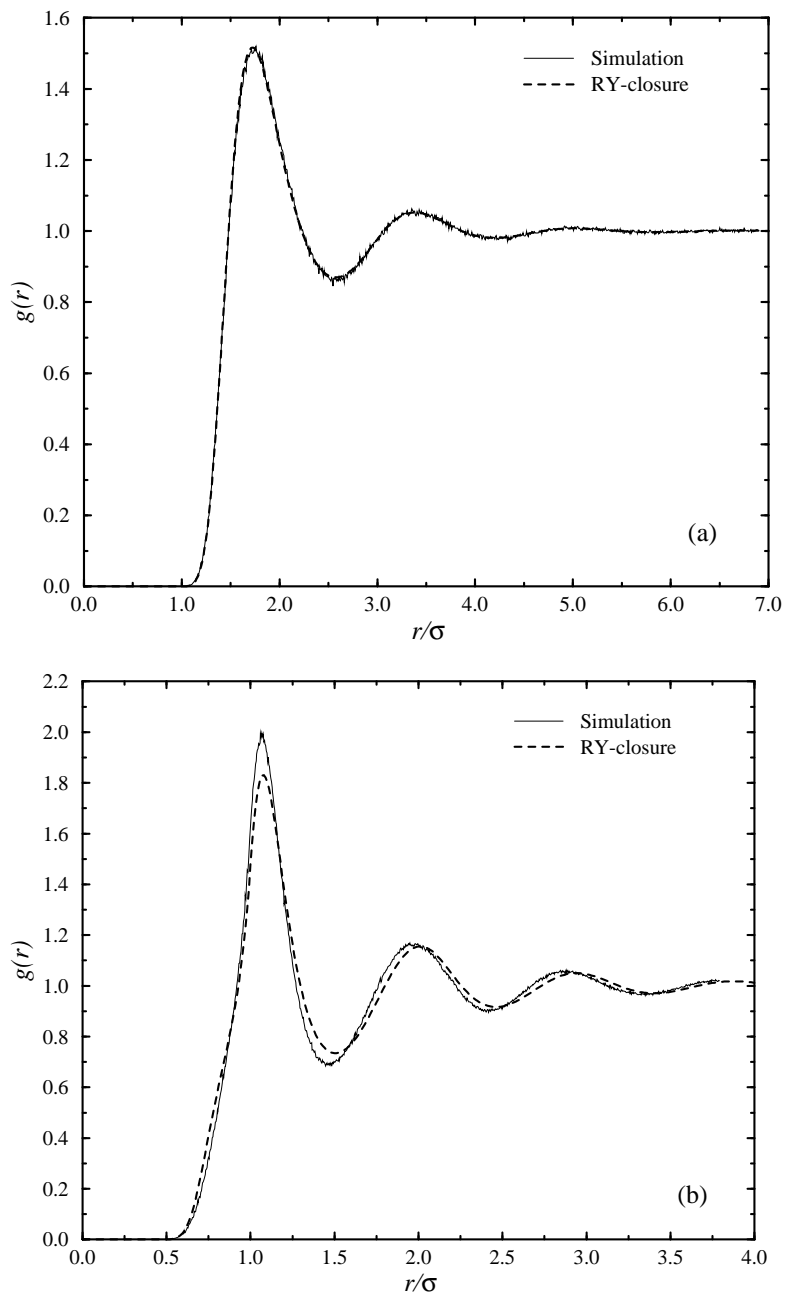
Figure 2. The radial distribution function $g(r)$ as obtained from simulations and from the RY closure for different η-values. (a) $\eta = 0.10$; (b) $\eta = 0.60$; (c) $\eta = 1.50$.

structure factor $S(k)$ which is simply ρ times the Fourier transform of the pair correlation function. The peaks of $S(k)$ reveal information about the characteristic length scales in the system. Alternatively, $g(r)$ is more appropriate if one wishes to determine, e.g., the average coordination number of the liquid.
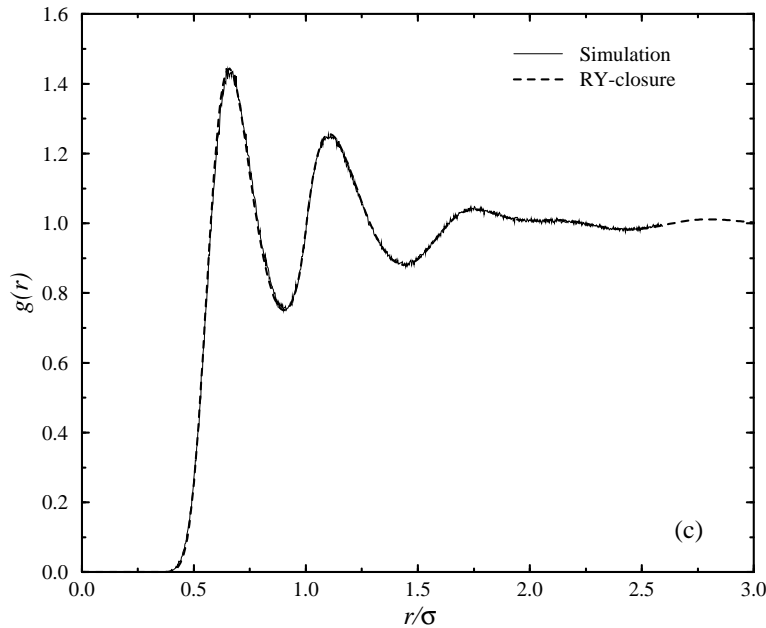
Figure 2. (Continued)

Both $g(r)$ and $S(k)$ can be measured in a standard Monte Carlo simulation [5, 6]. We have hence performed such simulations for a wide range of densities and, in addition, we have solved the Rogers–Young (RY) closure [11] in order to obtain a comparison. After ascertaining that the RY gives quite reliable results for all of the densities for which simulations were carried out, we relied on this closure to calculate the structure of the fluid for very high packings ($60.00 \gtrsim \eta \gtrsim 10.00$), where a simulation would be very expensive since a very large number of particles in the simulation box would be necessary in order to obtain reliable results.

In figure 2 we show representative results in order to provide a comparison of the radial distribution function $g(r)$ obtained from simulations with the RY result for various different values of η. Apart from small discrepancies for the intermediate value $\eta = 0.60$, it can be seen that the agreement is quite good. Hence, the RY closure is a reliable theoretical tool for the calculation of the pair structure of the liquid. It should also be noted that for high values of η, $\eta \gtrsim 3.0$, the RY closure reduces practically to the hypernetted chain (HNC) for our system. This is expected since, for high densities, we are dealing with a long-range interaction when distances are measured in units of average interparticle distance and the HNC is known to be most accurate precisely for long-range potentials.

The radial distribution function $g(r)$ of the system at hand shows the typical evolution of a normal liquid as the density is increased until we reach the overlap density ρ^*. This is the density at which the average interparticle distance $a = \rho^{-1/3}$ becomes equal to the length scale σ. It corresponds roughly to an overlap packing faction $\eta^* = 0.50$. For $\eta < \eta^*$, the function $g(r)$ displays oscillations with a characteristic length scale a. The heights of the peaks of $g(r)$ grow with density; the same behaviour is also observed for the structure factor $S(k)$, of course.

The situation changes above the overlap concentration, as can be seen in figure 3(a). Instead of having a main peak of $g(r)$ at $r \approx a$, we observe that one peak of $g(r)$ always
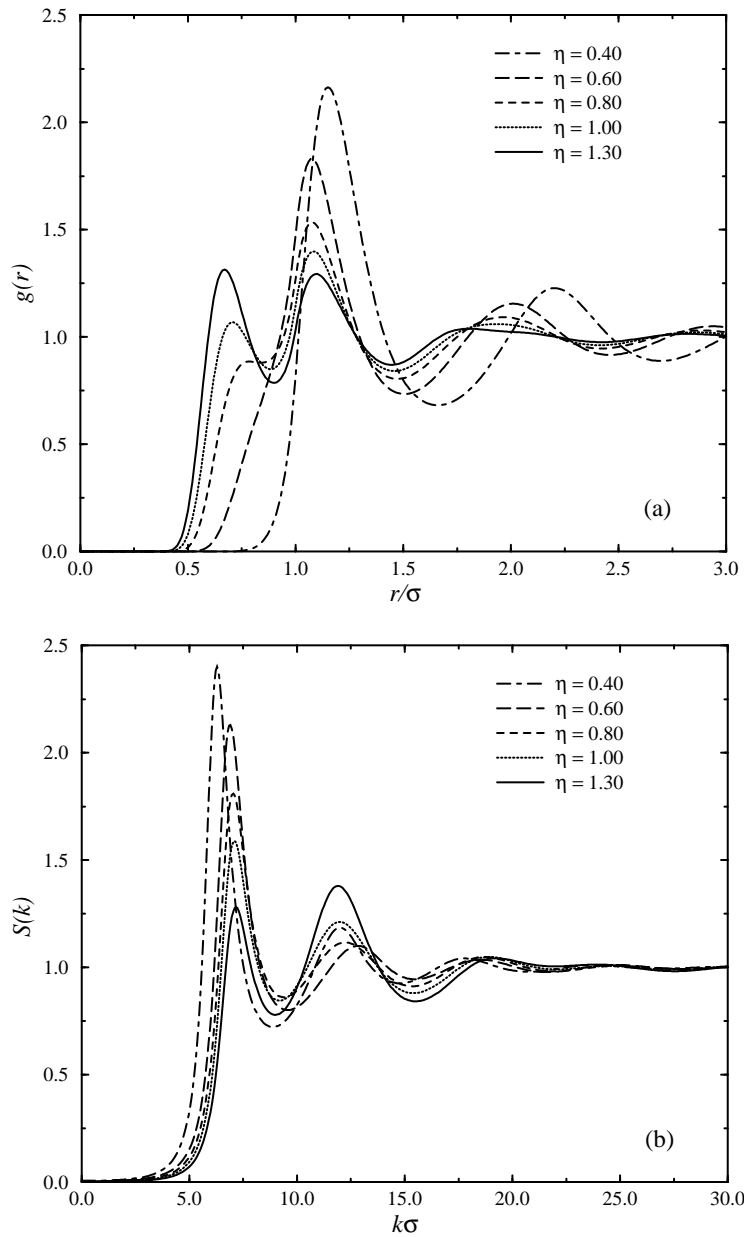
Figure 3. (a) The radial distribution function $g(r)$ and (b) the anomalous structure factor $S(k)$ above the overlap density.

remains at slightly outside the logarithmic part at $r \gtrsim \sigma$ *regardless of the density.* The 'main' peak of $g(r)$ grows gradually as the density is increased. Indeed, at $\eta = 0.80$, $g(r)$ shows just a shoulder preceding the peak at $r \gtrsim \sigma$ mentioned above and only at $\eta \geqslant 1.00$ can one distinguish a clear peak at $r \approx a$. Even then, this peak remains lower than the second until $\eta = 1.30$. Thereafter, it surpasses the second peak in height but, still, the position of the second peak of $g(r)$ is not at twice the distance of the first peak, as is the

case for normal liquids, because the latter is determined by the density and the former by the length scale σ.

This anomaly in $g(r)$ is reflected, naturally, in the shape and evolution of the structure factor $S(k)$, as can be seen in figure 3(b). As a first remark, we find that the height of the main peak of $S(k)$, which grows until we reach the overlap packing, becomes *lower* above η^*. More unusual features are observed if one looks at the positions and the competition between the first two peaks. Though the second peak remains at twice the position of the first up to $\eta = 0.60$, at packing $\eta = 0.80$ the position of the first peak is practically unchanged with respect to that at $\eta = 0.60$, but the second peak now *moves closer* to the origin and increases in height. This trend persists as η grows and already at $\eta = 1.30$ the second peak has become higher than the first, which shows a clear trend of disappearing at higher densities, as will be confirmed shortly.

This anomaly in the structure factor can be traced to the crossover of the interaction from a Yukawa to a logarithmic form *and* the softness of the logarithmic potential. Indeed, above the overlap concentration the system always 'tries' to maintain one coordination shell *outside* the logarithmic part, where the interaction is weak. At the same time, the softness of the logarithmic core allows two things to happen: on the one hand, qualitatively, the system always remains fluid which would not have been the case if the core was harder (e.g. a HS core, or even the same, logarithmic form for different f, as will be shown in section 4). On the other hand, more quantitatively, the softness of the logarithm allows for a rather broad first peak of the radial distribution function which can accommodate enough particles to allow for the second peak to occur immediately outside $r = \sigma$.

The unusual shape of the structure factor can be understood by means of the existence in $g(r)$ of these two different length scales: one length scale $a \approx \rho^{-1/3}$ which is manifestly density dependent and one length scale $b \gtrsim \sigma$ which is density independent. Below η^* only the first length scale appears but above η^* both are present. Let us call k_n the position of the nth peak of the structure factor. The first peak of $S(k)$ corresponds, roughly, to the length scale b, i.e. $k_1 \approx 2\pi/b$ and the second peak to the length scale $b - a$, i.e. $k_2 \approx 2\pi/(b-a)$. Indeed, as can be seen from figure 3(b), k_1 is practically constant, whereas k_2 decreases with density, a feature that can be attributed to the increase of the quantity $b - a \approx \sigma - \rho^{-1/3}$ with growing density. Moreover, the growth of the second peak can be understood since the structure that gives rise to it becomes more pronounced with increasing η, as the first peak of $g(r)$ takes shape.

In these terms, we can now make the hypothesis that the first peak of the structure factor will disappear altogether when the density is such that $b - a = a$ or $b = 2a$. In other words, the structure factor will have a main peak at a position dictated only by the density, when the length b is twice the length a, in such a way that $g(r)$ has exactly two oscillations of wavelength a between $r = 0$ and $r = b$. Since $b \approx \sigma$, it turns out that the density must be such that $a \approx \sigma/2$. As can be seen in figure 4(a) this occurs at the 'magic' value $\eta_2 = 3.40$, where the subscript denotes the number of oscillations of $g(r)$ in the interval $[0, b]$. Accordingly, the structure factor at $\eta = \eta_2$ has a strong first peak (which, however, has evolved from the second peak at lower densities!) located at a position $2\pi/a \approx 4\pi/\sigma$. In figure 4(b) we show also the structure factor at $\eta = 2.00$ in order to show the disappearance of what used to be the first peak of $S(k)$ and its replacement by the second one. However, we emphasize that the fact that at $\eta = \eta_2$ we have again a structure factor with its main peak located at a position $k_{max} \approx \rho^{1/3}$ does not mean that we are dealing with a normal liquid. Indeed, as can be seen from figure 4(b) the structure factor shows some weak substructure which is not present for usual liquids.

It is now pertinent to ask the question of what happens once the density is further
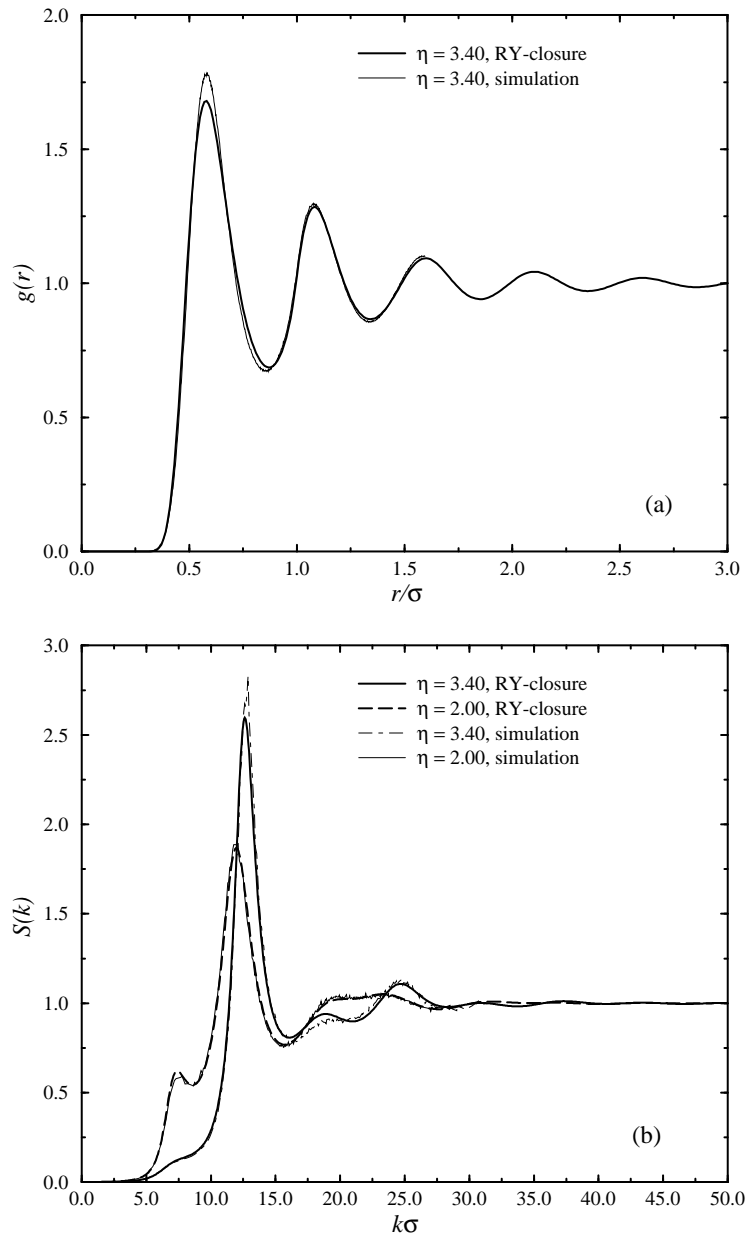
Figure 4. (a) The radial distribution function $g(r)$ and (b) the structure factor $S(k)$ as obtained from simulations and from the RY closure at $\eta = \eta_2 = 3.40$. For comparison, the structure factor at $\eta = 2.00$ is also shown.

increased. Does the height of the new main peak grow until the system solidifies or does the above scenario repeat itself? We have solved the RY closure for packing fractions up to $\eta = 60.00$ and we find that, in fact, it the second possibility that materializes. As η grows, the main peak is lowered and the one that used to be the third at low densities grows; see figure 5(a). The mechanism that brings about this scenario is none other than
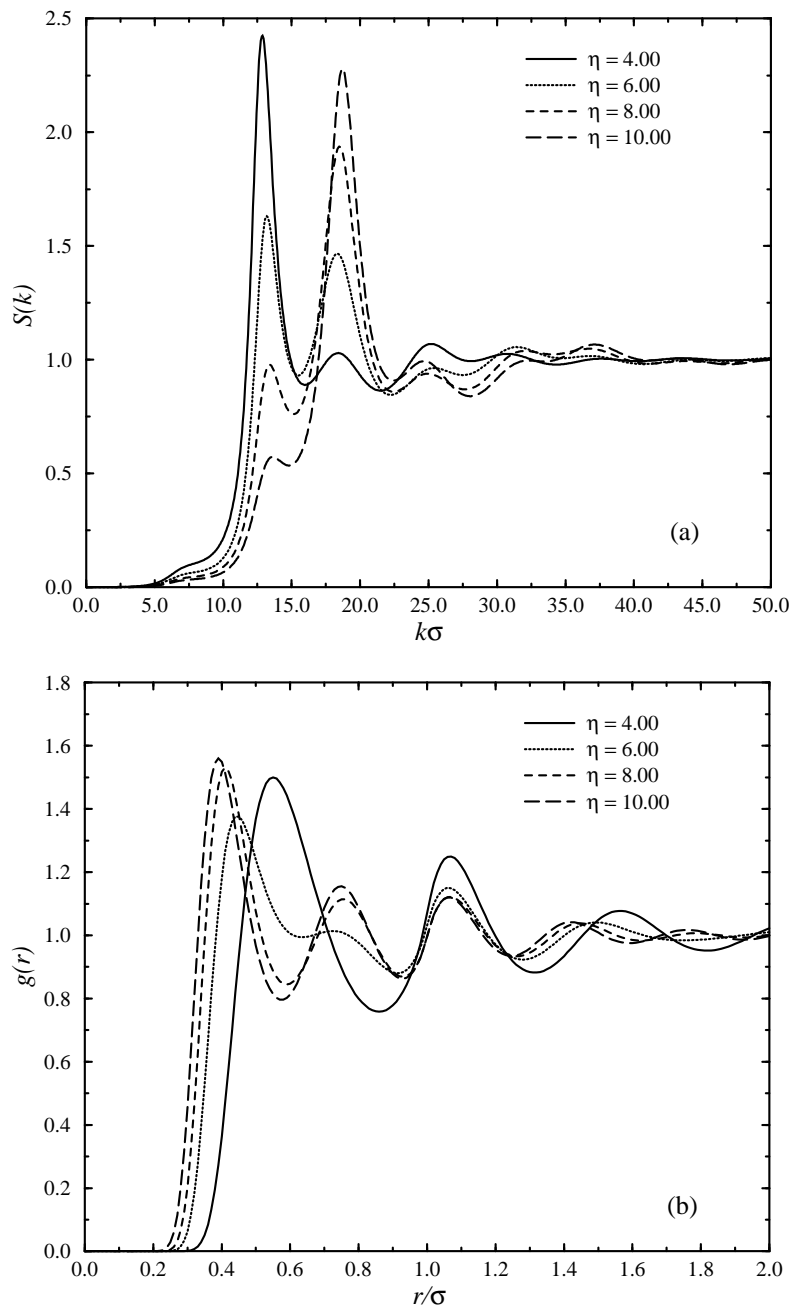
Figure 5. (a) The structure factor $S(k)$ and (b) the radial distribution function $g(r)$ for values of the packing fraction in the interval $\eta_2 < \eta < \eta_3$.

the development of more and more oscillations inside the logarithmic core in the function $g(r)$, as can be seen in figure 5(b). In fact, one can repeat the argument about the 'magic' packing fraction η_2 above for an arbitrary number of oscillations as follows: the structure factor $S(k)$ will be dominated by a single length scale whenever there is an integer number
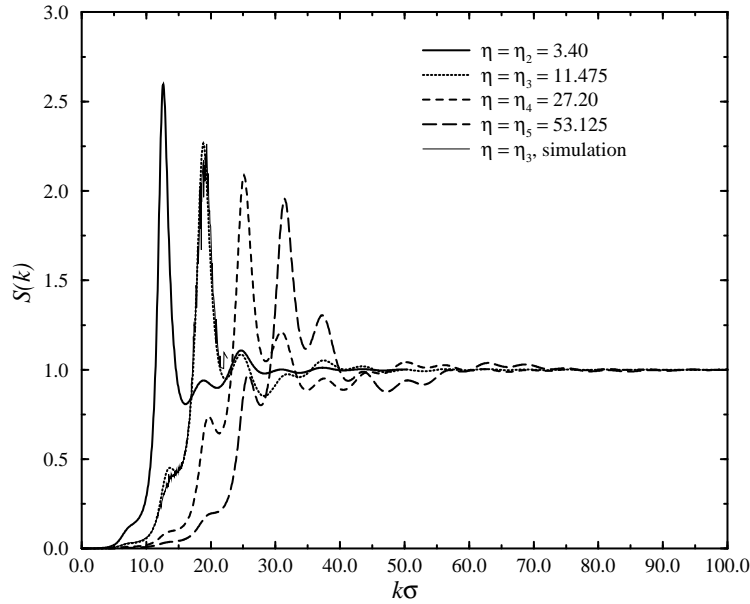
Figure 6. The structure factor $S(k)$ at the magic values of the packing fraction η_m, for $m = 2$, 3, 4 and 5.

of oscillations m between $r = 0$ and $r = b \approx \sigma$. Given the magic packing fraction η_2, it is straightforward to show that the general magic packing fraction η_m will be related to η_2 by

$$\eta_m = \left(\frac{m}{2}\right)^3 \eta_2 \qquad m = 3, 4, 5, \cdots. \tag{3}$$

Using $\eta_2 = 3.40$ we obtain $\eta_3 = 11.475$, $\eta_4 = 27.20$ and $\eta_5 = 53.125$. The structure factor for these magic values is shown in figure 6. It can be seen clearly that for the mth magic value, $S(k)$ has a dominant peak located at the position $2\pi m/\sigma$. As the order m grows, the height of the dominant peak also decreases slightly and some substructure develops in $S(k)$. However, the main length scale comes from the m oscillations of the radial distribution function $g(r)$ in the logarithmic core.

The above results can be nicely summarized by making a log–log plot of the positions of the first few peaks of the structure factor against the packing fraction η, as shown in figure 7. We emphasize here that when we talk about the nth peak we actually mean 'the peak which is the nth if we extrapolate at low enough densities that we are in a regime where the liquid is normal'. The reason for this distinction is that as η grows the low-order maxima of the structure factor disappear, as explained above, and as a result what used to be a second-order maximum now becomes first order etc. This is manifested in figure 7 by the fact that the curves representing the positions of the various maxima k_n stop at some value of η. Moreover, since a higher-order peak overtakes a lower-order one in height before the latter completely disappears, we indicate the highest peak in figure 7 by the filled symbols.

Referring to figure 7, we can make the following remarks: according to our previous definition, the fluid interacting by means of the potential given by equation (1) is normal for packing fractions $\eta \leqslant \eta^* = 0.50$. Indeed, in this regime on the one hand the first maxima follow the scaling $k_1 \propto \rho^{1/3}$ and on the other hand the higher-order maxima k_n are located at positions $k_n = nk_1$, both features being a manifestation of the existence of a *single* length
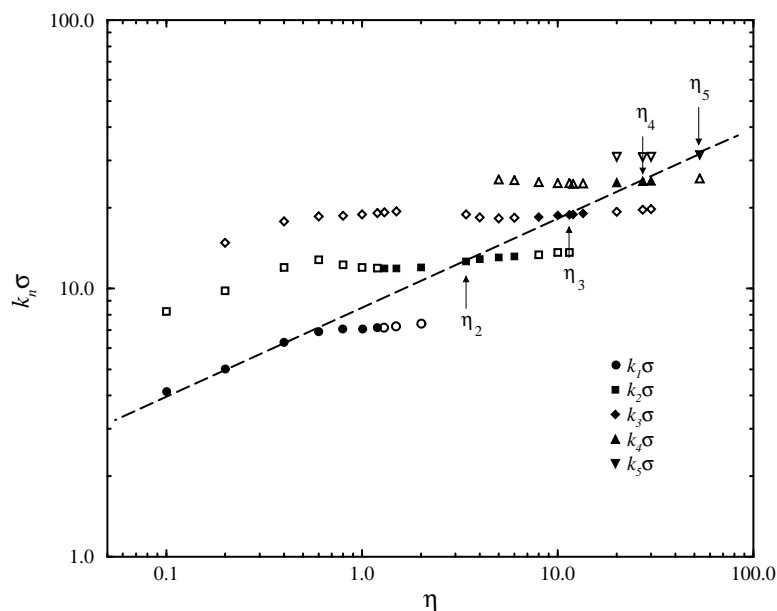
Figure 7. A log–log plot of the positions of the various peaks of $S(k)$ against the packing fraction η. The filled symbols indicate the highest peak (see the text). The arrows indicate the locations of the magic packing fractions η_m and the dashed straight line has slope 1/3.

scale $\rho^{-1/3}$ in the structure of the system. Above the overlap density ρ^* the scaling breaks down. However, if we extrapolate the straight line with slope 1/3 which characterizes the normal regime to higher densities, we find that it passes precisely through the main maxima at the magic packing fractions η_m. Indeed, at those values of the density the length scales $\rho^{-1/3}$ and σ are commensurate and we have an accidental scaling of the main peak of $S(k)$ with the one-third power of the density. However, the higher-order peaks of $S(k)$ are still not located at integer multiples of the first one and we are dealing with an unusual fluid for all densities exceeding the overlap density ρ^*.

4. Hard-sphere mapping and the freezing transition

The structure factors obtained for the whole range of densities have the characteristic that the maximum height of the main peak in $S(k)$ never exceeds the value 2.8. According to the empirical Hansen–Verlet criterion [12], a liquid freezes when the first maximum of the structure factor reaches a value 2.85. It was subsequently shown that freezing does indeed set in if the order in the liquid phase, as measured by the first maximum of $S(k)$, exceeds this quasi-universal value [13, 14]. Hence, we have a first indication that for $f = 32$ the system does not freeze. Naturally, the same must also hold for smaller f-values as the logarithmic core is then even softer. The absence of freezing was also confirmed in our numerical simulations, where for all values of η which were simulated ($\eta \leqslant 12.00$) the system remained in a liquid-like configuration, with any order parameter of a hypothetical crystalline solid vanishing.

Here, we want to apply a simple hard-sphere mapping procedure in order to corroborate the above results for $f = 32$ on the one hand and establish approximately the 'critical arm

number' f_c on the other; this is defined as follows: for $f \leqslant f_c$ the system remains fluid at all densities, but for $f > f_c$ there is at least one region in the density domain where the system is crystalline.

Following an idea of Kang *et al* [15], we define an effective hard-sphere diameter σ_{HS}, crudely representing the particle repulsion embodied in the pair potential of equation (1), as follows. The pair potential $V(r)$ is divided into a short-ranged reference potential $V_0(r)$ and a longer-ranged perturbation potential $W(r)$ at a suitably chosen break point λ. Thus, we write

$$V(r) = V_0(r) + W(r) \tag{4}$$

where $V_0(r)$ is given by

$$V_0(r) = \Theta(\lambda - r)\,[V(r) - F(r)]. \tag{5}$$

Here, $\Theta(r)$ is the Heaviside step function, and $F(r)$ will be defined soon. According to equations (4) and (5), the perturbation potential $W(r)$ is given by

$$W(r) = \Theta(\lambda - r)\,F(r) + \Theta(r - \lambda)\,V(r). \tag{6}$$

Now that we have split the potential in this way, it is possible to calculate the free energy of the system by a simple hard-sphere perturbation theory [15, 16]. In this theory, the potential $V_0(r)$ is used to calculate an effective hard-sphere diameter σ_{HS}, while the longer-ranged potential $W(r)$ is treated in a mean-field approach. In the following, we are not going to trace out calculations of free energies, but only to calculate σ_{HS}, which is density dependent when the specific choice for λ and $F(r)$, applied successfully in references [15, 16], is used. This density dependence arises from the identification of λ with the nearest-neighbour distance a_{fcc} of the fcc structure, i.e.,

$$\lambda = a_{fcc} \equiv \left(\frac{\sqrt{2}}{\rho}\right)^{1/3}. \tag{7}$$

Furthermore, the function $F(r)$ is chosen as

$$F(r) = V(\lambda) - \left[\frac{\mathrm{d}V(r)}{\mathrm{d}r}\right]_{r=\lambda} (\lambda - r) \tag{8}$$

guaranteeing that both $V_0(r)$ and $\mathrm{d}V_0(r)/\mathrm{d}r$ are vanishing at $r = \lambda$. With λ and $F(r)$ specified, σ_{HS} is then calculated from $V_0(r)$ by using the well-known Barker–Henderson (BH) approximation [17]

$$\sigma_{HS} = \int_0^\infty \mathrm{d}r \left[1 - \mathrm{e}^{-\beta V_0(r)}\right] \tag{9}$$

or, alternatively, by a scheme proposed by Weeks, Chandler and Anderson (WCA) [15, 16, 18]. We will only present results from the BH approximation, since the corresponding WCA results are practically identical to the latter, thus leading to the same conclusions.

After obtaining σ_{HS} from the BH or WCA scheme, we calculated the effective hard-sphere packing fraction

$$\eta_{HS} \equiv \frac{\pi}{6}\rho\sigma_{HS}^3$$

which is in general density dependent. We can hence plot η_{HS} as a function of the 'true' packing fraction η, depending furthermore on the value of f as an additional parameter. In figure 8, we show results for η_{HS} for five different functionalities f. Obviously, η_{HS} is increasing linearly with η for $\eta \lesssim 0.1$, and it reaches a maximum value depending on f at
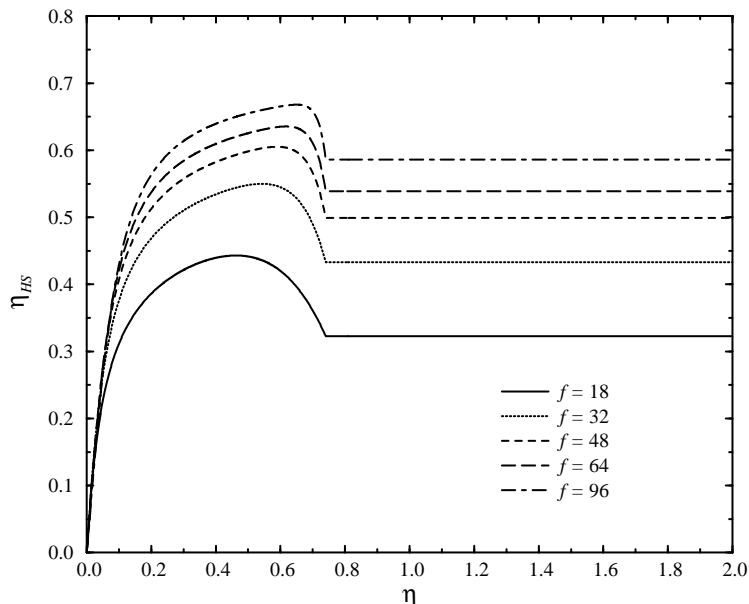
Figure 8. The effective hard-sphere packing fraction η_{HS} obtained by the procedure described in section 4 as a function of the true packing fraction η for five different values of the functionality f.

certain packing fractions $0.4 \lesssim \eta \lesssim 0.7$, which are again depending on f. For $\eta \geqslant 0.74$, η_{HS} remains constant for all densities.

We will now briefly explain this behaviour of $\eta_{HS}(\eta)$, before switching to some conclusions that can be drawn from figure 8 concerning the freezing transition of star polymers. For small η, where the break point λ is located at distances larger than the range of the pair potential, equations (5), (8) and (9) lead to a density-independent σ_{HS}, since the pair potential $V(r)$ is density independent. Hence, η_{HS} scales linearly with η in this regime. However, when λ reaches distances where the potential is remarkably different from zero, this linear scaling is no longer valid, since, according to equations (5) and (9), σ_{HS} is now a decreasing function with increasing density. This fact materializes in a decreasing slope of the function $\eta_{HS}(\eta)$, leading even to the existence of a maximum in $\eta_{HS}(\eta)$. Having these arguments in mind, the surprising fact that η_{HS} attains a constant value for $\eta \geqslant \eta_c = 0.74$ can be explained as follows. Exactly at the crossover packing fraction η_c, the break point λ is located at the corona diameter σ and thereafter, for $\eta > \eta_c$, we have $\lambda < \sigma$. Therefore, for $\eta \geqslant \eta_c$ the Yukawa part of the interaction potential $V(r)$ is irrelevant for the calculation of σ_{HS}, as the reference potential $V_0(r)$ is purely logarithmic. Using equations (1) and (9), it follows that in this regime σ_{HS} scales linearly with λ, i.e.,

$$\sigma_{HS} = \mathcal{A}(f)\lambda \tag{10}$$

with the constant $\mathcal{A}(f)$ depending only on the arm number f, but neither on σ nor on λ. Since λ scales with $\rho^{-1/3}$, equation (10) leads directly to the observed density independence of $\eta_{HS}(\eta)$ for $\eta \geqslant \eta_c$ [19].

The logarithmic pair interaction at hand is the only one showing this feature. Indeed, in order to have $\sigma_{HS} \propto \lambda$, the integrand in equation (9) must be a function of r/λ *only*, i.e., the length scale σ must drop out of the expression for $V_0(r)$. Let us assume that the pair

potential $V(r)$ is given by some function $R(r/\sigma; f)$ for $r \leqslant \lambda$. If the reference potential $V_0(r)$ has to depend on r/λ only, the function $R(x; f)$ must satisfy the following relations, as is clear from equations (5) and (8) above:

$$R(r/\sigma; f) - R(\lambda/\sigma; f) = \bar{R}(r/\lambda; f) \qquad \frac{dR(r/\sigma; f)}{dr} \propto \frac{1}{r} \qquad (11)$$

where $\bar{R}(x; f)$ is some other function. The above conditions (which are, in fact, not independent but equivalent to each other) are fulfilled only by the family of functions

$$R(x; f) = C(f) \ln(x) + D(f)$$

with $C(f)$ and $D(f)$ arbitrary.

We now turn to the main reason for our interest in the values of the effective hard-sphere packing fraction η_{HS}. Since the mapping onto an effective hard-sphere system gives quite reliable results in predicting the freezing transition [15, 16], we use the value of η_{HS} as an indication for the existence of a freezing transition in the original system. Hard spheres freeze in a fcc structure at $\eta_{HS}^{\text{solid}} = 0.55$ [20], and we therefore take this specific value to explore a possible freezing transition of star polymers from figure 8. Obviously, for $f \leqslant 32$, η_{HS} never exceeds 0.55 for all η, leading to the conclusion that the system remains fluid at *all densities*. For $f > 32$ on the other hand, η_{HS} attains values larger than 0.55 at least in a limited window of packing fractions η. Consequently, there is a critical arm number $f_c \simeq 32$, meaning that the system never freezes for $f \leqslant f_c$, but freezes presumably at least in a limited range of densities for $f > f_c$. Our previously described finding that star polymers with $f = 32$ did not freeze in all of our computer simulations is therefore consistent with this crude hard-sphere mapping procedure.

As can be further seen from figure 8, there is a range of arm numbers, $f_c < f \lesssim 64$, in which η_{HS} exceeds 0.55 only for $0.2 \lesssim \eta \lesssim 0.7$, which implies a 're-entrant-melting' phenomenon at $\eta \simeq 0.7$, i.e., a transition form a solid phase to a liquid phase if η is increased above 0.7. Here, it is worth mentioning that re-entrant melting for star polymer solutions at high concentrations was predicted by Witten *et al* on the basis of arguments arising from scaling theory [21]. This prediction is independently verified here. Moreover, within our crude model, star polymers with $f \gtrsim 64$ show a liquid phase for $\eta \lesssim 0.2$, followed by a solid phase for *all* higher densities.

5. Connection with experiments

From the experimental point of view, the extreme values of the packing fraction that we have considered in section 3 are unattainable. At most, one can expect to observe a change in the behaviour of the first peak of the structure factor as the overlap polymer concentration (which corresponds to our overlap density) is crossed. Our prediction is that the height of the first peak of the star–star structure factor of a star polymer solution in a good solvent is not monotonically increasing with polymer concentration but rather it saturates at the overlap density and decreases thereafter. On the basis of general scaling properties of polymers in good solvents, Witten *et al* predicted, more than ten years ago [21], precisely that the peak of $S(k)$ is largest when the separation between stars is of the order of the star radius. Here, we have confirmed this prediction quantitatively by employing a *colloidal* description of star polymer solutions. We expect that such effects should be visible in SANS experiments of dense star polymer solutions. To this end, stars with a labelled core should be used and the extent of the labelled part should be made as small as possible. In this way, the effects of increasing concentration on the structure factor will not be masked by the form factor of the single star.
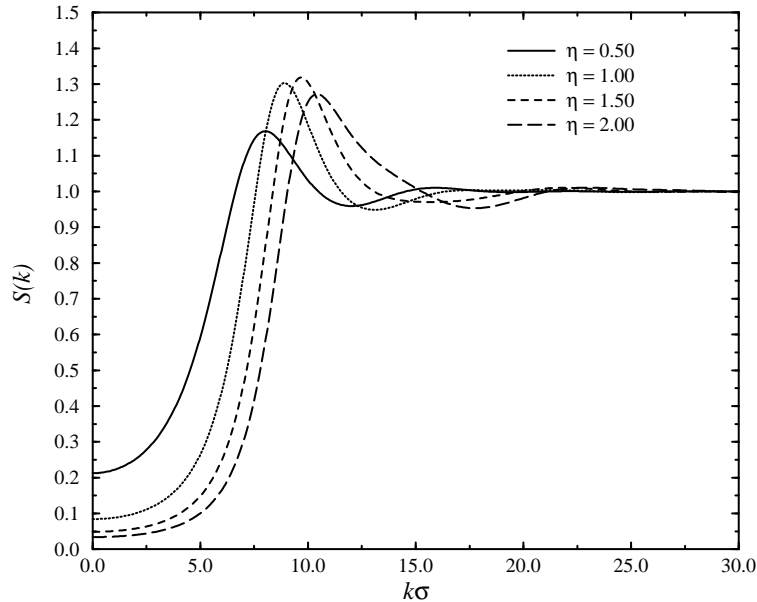
Figure 9. The structure factor of a system interacting by means of the potential given by equation (12) with $A = 10$ at various packing fractions η, obtained in the HNC closure. Notice the nonmonotonic behaviour of the maximum of $S(k)$ with increasing density.

Additionally, it is natural to ask whether this nonmonotonic behaviour in the peak of $S(k)$ is peculiar to the logarithmic form of the interaction inside the core or whether it can be seen for other functional forms of the pair potential as well. To test this, we have taken a toy potential which has a soft core for separations smaller than some length σ and a crossover to a different functional form for larger separations. This toy potential reads

$$\frac{\phi(r)}{k_B T} = \begin{cases} A(r - \sigma)^2/(r\sigma) & (r \leqslant \sigma) \\ 0 & (r > \sigma) \end{cases} \tag{12}$$

where A is some numerical constant which we can vary and controls the steepness of the interaction inside the core. We take now $A = 10$. Defining the packing fraction η as in equation (2) above, we have solved the HNC closure for a few different η-values. The results are shown in figure 9, where it can be seen that the same nonmonotonic behaviour of the main peak of $S(k)$ is observed. Thus, the phenomenon is rather general and it relies on the existence of a soft enough core in the interaction. Such interactions are not uncommon in soft-matter physics. Hence, it would be of great interest if such anomalies could be experimentally observed.

We finally comment on similarities of the logarithmic potential investigated in this work to a model introduced by Uhlenbeck and Ford in the early days of liquid-state theory [22]. This special model is defined by a Gaussian Mayer function

$$f(r) = 1 - \exp(-\beta V(r)) = \exp(-\alpha r^2)$$

corresponding to the pair potential

$$\beta V(r) = -\ln(1 - \exp(-\alpha r^2)).$$

As shown in reference [22], all interparticle correlations can be calculated analytically within the framework of graph theory. For small distances r, the above potential reduces to

$$\beta V(r) \simeq -2\ln(\sqrt{\alpha}r)$$

corresponding to the potential of equation (1) with an arm number $f = (36/5)^{2/3} \simeq 3.7$. Since this arm number is significantly smaller than f_c, we expect the model system of Uhlenbeck and Ford to be liquid for all densities, corresponding to an equation of state analytical in the density.

6. Summary and concluding remarks

Employing a pair potential which has been shown to describe correctly the SANS data of star polymer solutions in good solvents [3], we made quantitative predictions regarding the behaviour of the structure factor as a function of increasing polymer concentration. In particular, we found that above the overlap concentration, star polymer solutions display features which are unknown for normal liquids, namely a breakdown of the $\rho^{1/3}$-scaling of the positions of the peaks of $S(k)$ as well as an anomalous evolution of the heights of these peaks: the lower-order peaks diminish in height and the higher-order ones grow.

Furthermore, we applied a hard-sphere mapping and used it as a crude diagnostic tool in order to make preliminary investigations on the topology of the phase diagram of star polymer solutions. The most striking feature of the hard-sphere mapping procedure is, in our view, the fact that the effective HS packing fraction η_{HS} remains constant at high densities and depends only on the functionality f. We have shown that this characteristic is particular to the logarithmic interaction. We speculate that interactions which are softer than the logarithm will lead to an η_{HS} which will be a *decreasing* function of the density. This has relevance, in particular, to 'bounded' interactions, i.e., interactions which do not diverge at the origin, such as the Gaussian potential of Stillinger and Stillinger [23] or a simple model of penetrable spheres introduced recently by us [24].

Another question of great interest is the phase diagram of star polymers. Detailed calculations, based on extensive computer simulations as well as perturbation theory, are currently under way. These calculations allow for the evaluation of the Helmholtz free energies of various candidate crystalline phases and, subsequently, the comparison of the latter with that of the fluid phase and the construction of the phase diagram. Preliminary results are in full agreement with those presented here as far as the critical arm number f_c is concerned; at the same time, they reveal a rich topology of the phase diagram as well as a variety of unusual crystal structures. The presentation of the phase diagram of star polymers will be the subject of a future publication.

Acknowledgment

References

[1] Daoud M and Cotton J P 1982 *J. Physique* **43** 531
[2] Grest G S, Fetters L J, Huang J S and Richter D 1996 *Adv. Chem. Phys.* **94** 67
[3] Likos C N, Löwen H, Watzlawek M, Abbas B, Jucknischke O, Allgaier J and Richter D 1998 *Phys. Rev. Lett.* **80** 4450
[4] Hansen J-P and McDonald I R 1986 *Theory of Simple Liquids* 2nd edn (New York: Academic)

[5] Allen M P and Tildesley D J 1987 *Computer Simulation of Liquids* (Oxford: Clarendon)
[6] Frenkel D and Smit B 1996 *Understanding Molecular Simulation* (London: Academic)
[7] The blob picture of a star is described in reference [1].
[8] Witten T A and Pincus P A 1986 *Macromolecules* **19** 2509
[9] Triplet forces start to become relevant only if three spheres of diameter σ exhibit a triple overlap within their corona, corresponding roughly to densities $\rho > 2\rho^*$.
[10] Buitenhuis J and Förster S 1997 *J. Chem. Phys.* **107** 262
[11] Rogers F A and Young D A 1984 *Phys. Rev.* A **30** 999
[12] Hansen J-P and Verlet L 1969 *Phys. Rev.* **184** 151
[13] Hansen J-P and Schiff D 1973 *Mol. Phys.* **25** 1281
[14] Löwen H 1994 *Phys. Rep.* **237** 249
[15] Kang H S, Lee C S, Ree T and Ree F H 1985 *J. Chem. Phys.* **82** 414
[16] Lutsko J F and Baus M 1991 *J. Phys.: Condens. Matter* **3** 6547
[17] Barker J A and Henderson D 1967 *J. Chem. Phys.* **47** 4714
[18] Weeks J D, Chandler D and Anderson H C 1971 *J. Chem. Phys.* **54** 5237
[19] Notice that the specific value of η_c observed here, is a consequence of the identification of λ with a_{fcc}, resulting in $\eta_c = 0.74$, which is the maximum packing fraction for a fcc crystal of hard spheres. If, e.g., λ is identified with the nearest-neighbour distance in a bcc crystal, $\eta_c = 0.68$. Nevertheless, all of the features of $\eta_{HS}(\eta)$ described remain the same.
[20] Bolhuis P G, Frenkel D, Mau S-C and Huse D A 1997 *Nature* **388** 235
[21] Witten T A, Pincus P A and Cates M E 1986 *Europhys. Lett.* **2** 137
[22] Uhlenbeck G E and Ford G W 1962 *Studies in Statistical Mechanics* ed J De Boer J and B E Uhlenbeck (Amsterdam: North-Holland)
[23] Stillinger F H and Stillinger D K 1997 *Physica* A **244** 358 and references therein
[24] Likos C N, Watzlawek M and Löwen H 1998 *Phys. Rev.* E at press